Volume 8
Print Reference: Pages 287-305

Article 37

2018

Understanding How the Flood Sediment Record Was Formed: The Role of Large Tsunamis

John Baumgardner
Logos Research Associates

Baumgardner, J. 2018. Understanding how the Flood sediment record was formed: The role of large tsunamis. In *Proceedings of the Eighth International Conference on Creationism*, ed. J.H. Whitmore, pp. 287–305. Pittsburgh, Pennsylvania: Creation Science Fellowship.

UNDERSTANDING HOW THE FLOOD SEDIMENT RECORD WAS FORMED: THE ROLE OF LARGE TSUNAMIS

John Baumgardner, Logos Research Associates, 24515 Novato Place, Ramona, CA 92065, johnrbaumgardner@gmail.com

ABSTRACT

A daunting challenge for Flood geology is providing a credible explanation for how the staggering volume of fossil-bearing sediment was eroded, transported, and deposited in orderly patterns on the surface of the normally high-standing continents in only a few months' time. This paper applies numerical modeling to explore the question of whether repetitive giant tsunamis generated by catastrophic plate tectonics during the Genesis Flood can plausibly account for the Flood sediment record. The modeling suggests with reasonable parameter choices that tsunami-driven erosion during the Genesis Flood can produce considerable volumes of new sediment, that tsunami-driven pulses of turbulent water can transport this sediment vast distances across the continental surfaces, and that these hydrological processes generate sequences of laterally extensive layers often separated by erosional unconformities. The model incorporates a representation of the dynamic history of the continental blocks to explore the consequences of continental motions. It also includes an initial continental topography, with low elevations along the coasts and higher elevations inland. This computational study provides important insight regarding the primary source of the Flood water, how that water was able to cover the normally high-standing continent surface, what produced and sustained the water flow, primary sources of the sediment, primary means of sediment transport and deposition across the continent surface, why so little erosional channeling occurred between sediment layers, processes responsible for observed paleocurrent directions, and mechanisms responsible for the abundance of planar erosional features at many scales. It is vital to stress that the exploration described in this paper is still exceedingly limited in its realism relative to the actual earth and includes only a restricted subset of the processes in operation during the Flood cataclysm. Despite the limitations, it suggests strongly that tsunamis likely played a key role in producing the fossil-bearing sediment record we observe today.

KEY WORDS

Genesis Flood, giant tsunamis, catastrophic plate tectonics, turbulent sediment transport, open channel flow, cavitation erosion, shallow water approximation

INTRODUCTION

A central challenge for Flood geology is providing a credible explanation for how the staggering volume of fossil-bearing sediment was eroded, transported and deposited in orderly patterns on the surface of the normally high-standing continents in only a few months' time. Some of the prominent issues are the source of the Flood water, how that water came to cover the normally high-standing continent surface, the sources of the sediment, the nature of the water flow that transported and deposited the sediment across the continent surface with surprisingly little erosional channeling of the sediment layers, the mechanism responsible for producing and maintaining that water flow, the cause for the abundance of planar erosional unconformities at many scales in the sediment record, and where the Flood water went at the end of the cataclysm.

The daunting complexity of this task prompted the author about seven years ago to pursue a numerical modeling strategy in a beginning attempt to address the task. Two previous papers (Baumgardner 2013; Baumgardner 2016) have documented the mathematical underpinnings and numerical methods in moderate detail. In brief, the approach is to solve for the water flow across the earth's surface utilizing what are known as the shallow water equations that enforce conservation of mass and a balance of forces on each cell in the computational grid. The shallow water equations are a version of the standard Navier-Stokes equations for fluid flow that make the simplifying assumption that fluid depth is small compared with the horizontal scales of interest. The shallow water equations allow one to treat the water as a single layer with laterally varying surface height above laterally varying bottom topography. In addition, over continental regions, where the water depths are much smaller relative to the deep ocean and where turbulence can be expected to arise because of high water velocities, the equations of open channel flow are solved to track the suspension, transport, and deposition of any sediment present. Erosion is treated assuming that cavitation is the dominant mechanism under the conditions that prevailed during the Flood.

1. Potential causes of the water motion during the Flood

Even with all this numerical machinery in place and working, a prominent issue remains, namely, what was it that drove the water motion? In the investigations leading to the Baumgardner (2013) paper, several possibilities were explored, including bolide impacts in the ocean, torque from a close approach of a planetary body, and the tidal effects of such a close encounter. Of these three possibilities, it was found that only the third can drive the water flow strongly enough and over a large enough fraction of the earth's surface to generate sufficient sediment and distribute it over the land surface in any sort of pattern that might bear some resemblance to the actual sediment record. Even in that case it was necessary to postulate multiple near approaches, presumably by the same extraterrestrial body, during the time span of the Flood.

Following the presentation of that paper at the 2013 ICC, a colleague inquired if I had considered tsunamis produced by catastrophic plate tectonics during the Flood as a possible driving mechanism. Although I had briefly considered this possibility, I had dismissed it because I had thought the tsunami amplitude would be too small. However, prompted by my colleague's inquiry, I reexamined the idea and realized that, if during the Flood the overriding plate locks witht the subducting plate, even for a few minutes, when the plates unlock and slip, a huge tsunami would result. I further realized that given the total length of the subduction zones that had to be active during the Flood, the total number of such large tsunamis would have been large and their frequency quite high.

A simple analysis showed that with plate speeds on the order of 2 m/s, a subduction angle of 45°, and a plate locking interval of 60 minutes, the sea bottom is depressed by more than 5 km. When the plates then unlock and slip, the seafloor rebounds toward its undepressed state, launching a gigantic tsunami easily capable of traversing a supercontinent. Moreover, if even half the length of subduction zones active in the present world were active at any given time during the Flood, that implies some 25,000 km of active zones. If the average segment length where slip occurs in a single event is 1500 km, and if the locking interval is one hour, this implies an event every four minutes. This is equivalent to 15 events per hour, 360 per day, or 54,000 in a span of 150 days. I realized that this represented a potent mechanism for driving high velocity water motion during the Flood deserving careful investigation. Implementing this new feature in the numerical model was not difficult.

2. Large amplitude, high frequency tsunamis yield unexpected consequences

As I explored the response of the model with new mechanism for driving water flow, I observed striking new behavior I had not seen previously. I noticed that, as the tsunamis initially surged over the land surface, the water levels not only began to rise but that water levels continued to rise until the continent surface everywhere was deeply flooded. I also observed that the Coriolis effect was strongly influencing the pattern of flow, with strong anti-cyclonic gyres appearing at high latitudes where the Coriolis effect was greatest. The largest water depths were at the centers of these anti-cyclonic gyres. Simple analysis revealed that the Coriolis force associated with the circular water motion was balancing the force from the height gradient of the water piled up beneath the gyre. Emplacement of water onto the continent surface by the tsunami pulses was compensating for runoff from gravity, thereby maintaining the piles of water and the circular pattern of water flow.

I realized that this mechanism of repetitive tsunamis provided a rather simple answer to the longstanding puzzle as to how the normally high-standing continents were covered by water for months during the Flood. The answer is that the repetitive large tsunamis were emplacing seawater onto the land surface and thereby compensating for the tendency of runoff due to gravity.

Not only did early numerical experiments reveal this tendency for the continental surface to flood quickly and remain flooded as long as the large-amplitude tsunamis continued, it also demonstrated their potency for eroding the continental bedrock, particularly along the continent margins. In addition, the early numerical experiments demonstrated the adequacy of the mechanism for suspending, transporting, and distributing vast quantities of sediment over the continental surface. I subsequently published results from these experiments for two stationary continent configurations (Baumgardner 2016). The first case was a circular supercontinent centered on the equator with a smooth, almost flat surface that covered 38% of the earth, with the remainder of the earth covered with deep ocean. The continent geometry was almost identical to that utilized in Baumgardner (2013). The second case was similar except that the supercontinent shape resembled Pangea. In both cases, the continent surface was quickly flooded by the tsunamis and the flooding persisted as long as the tsunamis were allowed to continue. In addition, relatively stationary anti-cyclonic circulation patterns quickly appeared at high latitudes in both hemispheres from the Coriolis effect. The greatest elevations of the water surface and greatest depths of accumulated sediment were associated with these gyres. As might be expected most of the erosion and sediment generation occurred along the continent margins due to the impinging tsunamis.

While these beginning calculations with tsunamis did show promise in being able to account for some of the most crucial aspects of a global Flood as described in Genesis, the sediment patterns in these simple calculations displayed little resemblance to those that blanket the continents today. It was clear that much more realism was needed before the sediment patterns in the model could possibly show even a remote correspondence with the actual record. Therefore, I undertook additional effort to address that need. Much of that effort involved replacing the static continent configuration with a treatment that tracks the breakup of a pre-Flood supercontinent, the reassembly of the resulting blocks into a Pangean supercontinent, the subsequent breakup of that supercontinent and dispersal of its resulting blocks, and their movements to their present locations. I also included a history, based on paleomagnetic observations, of the changing orientation of the earth's spin axis relative to the continents during the Flood. Tracking the history of the spin axis orientation is important because it controls the spatial expression of the Coriolis effect. Finally, I also added a more realistic topography to the continental surfaces, with a gradual increase in topographic height from -200 m along the coastlines to 1,000 m elevations in the continental deep interiors.

3. Discovery of a numerical artifact responsible for the persistent continental flooding

As I explored the behavior of this enhanced version of the model, specifically the water flow directions on the continents with the more realistic topography, I noticed a disturbing pattern. I found the water flow was consistently downslope. With a bit of sleuthing I found the cause to be a problem in the numerical formulation. In numerical models that involve fluid flow, accuracy is critical in how fluid is transported from one cell to the next. Because of its inherently small amount of numerical diffusion, I had elected to use what is known as a semi-Lagrangian transport method. Even though the amount of anomalous numerical diffusion is much smaller in this method than in most others, its downside is that it is not perfectly mass-conserving. To guarantee mass conservation, I

had chosen a simple strategy. On each time step I simply added or subtracted a tiny uniform correction to the water depth to enforce mass conservation.

Upon checking, however, I discovered that the cells in which the mega-tsunamis were being generated displayed mass-conservation errors substantially larger than I had anticipated. I further discovered that these errors consistently involved a water deficit. Hence, the corrections that were being applied were consistently positive ones that added a modest amount of water to the continent surfaces on each time step. It was immediately clear to me that these consistently positive corrections were the explanation for the unexpected continental flooding I had reported in the 2016 paper and also for the consistent downslope water flow I observed in the model with more realistic continental topography. I found that this problem could be alleviated through two relatively small changes in the formulation. The first change involved correcting most of the large errors associated with the tsunamis locally within the cells in which they occurred. The second involved applying a consequently much smaller water depth correction over regions of deep ocean where the water depths were large and no depth correction at all over continental regions. This strategy stably conserved water volume and eliminated the tendency for anomalous flooding of the continents.

I plan soon to re-run the calculations reported in the 2016 paper and to post the revised results as a correction. I am grateful to have identified this numerical problem before submitting this paper. The purpose of this paper then is to document the results from the enhancements in the numerical model outlined in the preceding section.

BACKGROUND

As already stated, accounting for the generation of the continental fossil-bearing sediment record in terms of the Genesis Flood, especially with its brief time span, is by no means a trivial task. In continental platform regions, such as the heartland of the U.S., the thickness of the fossil-bearing sediment sequence commonly exceeds 2,000 m (Prothero and Schwab 2004). Moreover, individual formations typically display amazing horizontal continuity, in some cases spanning multiple continents (Ager 1973). The physical processes responsible for generating such an enormous volume of sediment and then transporting and depositing it in such orderly, laterally extensive layers—all within a few months as the Biblical text indicates—staggers the mind to imagine.

Just how much sediment was processed by the Flood? Various approaches have been applied to estimate the earth's current sediment inventory. Prothero and Schwab (2004) summarize some of these estimates. One mentioned by these authors and quoted by several others is that of Pettijohn (1975) equal to 5% of the earth's total crustal volume. Since crustal thickness averaged over both oceanic and crustal regions is 16 km, Pettijohn's estimate corresponds to a global spherical layer 800 m in thickness. Prothero and Schwab (2004) provide the range of 800-1,000 m as their own estimate for the mean global sediment thickness that can be derived from direct measurements (as opposed to estimates based on ocean chemistry). It is further helpful to know how this sediment inventory is partitioned between deep ocean and continent. Olson *et al.* (2016), in a compilation involving some 10 million separate oceanic sediment thickness determinations, obtained a value of 418 m as the current average oceanic sediment thickness. The oceanic area for their study spanned 71% of the earth's surface. Partitioning the balance of the sediment inventory to the continents yields an average continental thickness of 1,735 m when the global average is assumed to be 800 m and 2,025 m when it is assssumed to be 1,000 m. Some portion of the continental inventory corresponds to Precambrian or pre-Flood sedimentary rocks, but probably not more than 10%. To summarize, a reasonable estimate for the volume of sedimentary rock deposited during the Flood corresponds to a layer approximately 1,000 m thick, or perhaps a bit less, over the entire earth.

What about the *rates* required for the erosion, sediment transport, and deposition during the Flood? Rough estimates of these are relatively simple to obtain. Assuming most of the primary deposition occurred within the interval of 150 days during which "the water prevailed on the earth" (Genesis 7:24), one can find the average deposition rate over that interval required to give the average sediment thickness of 2,000 m over the continents today. Dividing 2,000 m by 150 days yields an average rate of deposition of 13.3 m/day (0.56 m/hr or 1.5×10^{-4} m/s). This also suggests a comparable average rate of erosion, at least to supply the continental sediment.

Not only does the brief time span of the Flood require the erosion and deposition rates to be high, but the large horizontal extent of the layers demands that the transport times for individual sediment particles be large as well. If one assumes that the average distance between the sites of erosion and deposition is 500 km (5×10^5 m) and an average speed of transport by moving water of 20 m/s (45 mph), then a typical sediment particle must be carried along for $(5 \times 10^5 \text{ m})/(20 \text{ m/s}) = 2.5 \times 10^4$ s, or 6.9 hr. One can further inquire as to the amount of sediment being suspended and transported by the flow to achieve the required erosion/deposition rate. The answer is simply the product of the average erosion/deposition rate and the transport interval, $(1.5 \times 10^{-4} \text{ m/s}) \times (2.5 \times 10^4 \text{ s}) = 3.8$ m.

If the transport is solely by turbulent suspension, observations show that the carrying capacity of the water column is limited to 5-10% sediment volume concentration (Pierson 2005). This limit implies that a turbulent water column 38-76 m thick is needed to keep 3.8 m of sediment in turbulent suspension. At sediment concentrations greater than 5-10%, the sediment begins to modify the flow behavior from that of turbulent water toward what is known as the hyperconcentrated flow regime (Pierson 2005). At this stage in the development of the model, the transport is restricted to that of turbulent suspension and it is assumed that whenever sediment volume concentrations in the sediment column exceed 10% the excess sediment comes out of suspension and is deposited on the land surface. These simple estimates suggest that turbulent water several tens of meters deep moving at velocities of tens of m/s must have been the norm over the continental surface during the initial months of the Flood. Since these are time-averaged estimates, when the likelihood of significant time variation is taken into account, the peak water depths and speeds must have been substantially higher.

APPROACH

This paper assumes that tsunamis generated by the locking and subsequent slip of the plate that overrides rapidly subducting lithospheric slabs in oceanic subduction zones was the primary mechanism for driving water motion during the Flood. In today's world, the overriding plate is stuck and locked at a subduction zone against the continuously subducting oceanic plate except for short interludes of rapid unlocking and slip. As documented by GPS

measurements, this locking and episodic unlocking and slip of the overriding plate takes place even as the subducting plate is moving continuously downward into the mantle below. Relative motion between the subducting plate and overriding plate occurs only during these extremely brief episodes as the two plates suddenly unlock and slide rapidly past each other. In almost all cases today the episode of slip produces an earthquake and often also a tsunami. In the context of the Flood, when the plates were moving approximately a billion times faster than they are at present, a crucial issue is the nature of the subduction zone mechanics. Currently, no one has yet undertaken a careful numerical investigation of the dynamics in these zones under such conditions. Despite the consequent uncertainties, the approach taken in this study is to assume that subduction zone behavior during the Flood resembled that of today. That assumption is likely to be valid if during the Flood the plates remained cool enough to behave elastically and therefore stored substantial elastic energy as they do today. To me that is plausible.

Studies of plate motions during the Flood yield plate speeds on the order of 2 m/s (Baumgardner 1994; Baumgardner 2003). Using that horizontal speed for the subducting plate and assuming a subduction angle of 45° implies that the ocean bottom in the subduction zone is being pulled downward at a speed of 2 m/s sin (45°) = 1.4 m/s. If the locking persists for 96 minutes (5,760 s), the sea bottom is depressed by more than 8,000 m. Sudden unlocking and slip between the overriding plate and the subducting plate will cause the sea bottom to rise by that height, unleashing a huge tsunami. Globally during the Flood, it is likely that subduction zones were comparable in linear extent as today, on the order of 50,000 km. If, as shall be assumed, at any given time there are only 16 active subduction zone segments, each 1,500 km in length, for a total active length of 24,000 km, and if each of these segments locked and slipped every 96 minutes, this would imply 10 mega-tsunamis unleashed each hour, 240 each day, and 36,000 over the course of five months in the world's ocean basins. These are the tsunami parameters assumed for the calculation reported in the results section below. However, the length of the zones that unlock and slip in today's world typically is much less than 1,500 km. If, in reality, during the Flood it was only 750 km on average, then keeping the locking time the same would increase the total number of events to 480 each day and 72,000 over a span of five months.

The erosive power of these waves as they strike the continental margins and then race largely unhindered across the continental surface is difficult for the human mind to imagine. The turbulence where the water is relatively shallow over the continental surface is strong enough to maintain many tens of m of sediment in suspension. Turbulence is the physical mechanism that enables the suspension and makes possible the long-distance transport of the sediment. Subsequent discussion of the numerical results reveals that these processes are readily adequate to account for major aspects of the Flood sediment record.

1. Mathematical framework

Prominent features of the sediment record suggest that sheets of turbulent water sweeping over the continent surface must have played a key role. Such water motion is in the general category of turbulent boundary layer flow, which is one of great practical interest and one that has been studied experimentally for many years. In the hydrologic engineering community, this type of water flow is referred to as open channel flow. Examples of open channel flows include rivers, tidal currents, irrigation canals, and sheets of water running across the ground surface after a rain. The equations commonly used to model such flows are anchored in experimental measurements and decades of validation in many diverse applications. It is the turbulence of the flowing water in such flows that keeps the sediment particles in suspension. The *Journal of Hydraulic Engineering* is but one of several journals that has published a wealth of papers on turbulent open channel flow and sediment transport over the past many decades.

Appendix A in Baumgardner (2016) summarizes the observations, experiments, and efforts to formulate a mathematical description of fluid turbulence over the past two centuries. A description of turbulent fluid flow provided almost a century ago by the British scientist L. F. Richardson (1920) is still valid today. His description is a flow whose motions are characterized by a hierarchy of vortices, or eddies, from large to tiny. These eddies, including the large ones, are unstable. The shear that their rotation exerts on the surrounding fluid generates smaller new eddies. The kinetic energy of the large eddies is thereby passed to the smaller eddies that arise from them. These smaller eddies in turn undergo the same process, giving rise to even smaller eddies that inherit the energy of their predecessors, and so on. In this way, the energy is passed down from the large scales of motion to smaller and smaller scales until reaching a length scale sufficiently small that the molecular viscosity of the fluid transforms the kinetic energy of these tiniest eddies into heat.

When a fluid is moving relative to a fixed surface, the speed of the fluid, beginning from zero at the boundary, increases—first rapidly, and then less rapidly—as distance from the surface increases. The region adjacent to the surface in which the average speed of the flow parallel to the surface is still changing, at least modestly, as one moves away from the surface is known as the boundary layer. When the speed of the fluid over the surface is sufficiently high, the boundary layer becomes turbulent and becomes filled with eddies that can span a broad range of spatial scales. Appendix B in Baumgardner (2016) summarizes some of the prominent features of turbulent boundary layers, including the discovery that the mean velocity profile within the turbulent boundary layer is very close to a logarithmic function of distance from the boundary. Remarkably, the parameters specifying the profile can be determined merely from the thickness of the layer and its mean flow speed.

The theory of open channel flow applies this mathematical representation of a turbulent boundary layer to describe sediment suspension, transport, and deposition by turbulent water flow for cases where the width of the flow is much greater than the water depth. Appendix C in Baumgardner (2016) provides the derivation of a mathematical expression for the sediment carrying capacity of a layer of turbulent water as a function of sediment particle size. This expression is utilized in the numerical treatment to quantify the sediment suspension of the water flow. The expression requires the particle settling speed for each of the particle sizes that is assumed in the model. Appendix D in Baumgardner (2016) describes how these settling speeds may be obtained via empirical fits to experimental data.

Obviously, a prominent issue in the formation of the earth's sediment record is the origin of the sediment. From the rock record it is clear that there were pre-Flood continental sediments. However, for sake of simplicity, these sediments are ignored in the current version of the model. Instead, it is assumed that all the sediment deposited is derived from erosion of continental bedrock. In terms of erosional processes, I restrict the scope to the mechanism of cavitation,

again for simplicity. I suspect, however, that contributions from other processes by comparison were small. I further assume that the cavitation erosion of crystalline continental bedrock results in a distribution of particle sizes corresponding to 70% fine sand, 20% medium sand, and 10% coarse sand. Here the fine sand fraction also includes the clay and silt, which are assumed to flocculate to form particles that display settling behavior identical to that of fine sand. Mean particle diameters for these three size classes are 0.063 mm, 0.25 mm, and 1 mm, respectively. In this model I neglect carbonates which in the actual rock record represent on the order of 30% of the total sediment volume.

I recognize that it is difficult to imagine how feldspar, even when reduced by cavitation to 0.063 mm particle sizes and smaller, might be transformed to clay minerals in the brief time span available during the Flood. I acknowledge that a significant portion of the clay in the shales and mudstones in the Phanerozoic sediment record may well have been derived from shales and mudstones of the pre-Flood earth. For example, the Precambrian tilted strata exposed in the inner gorge of the Grand Canyon, rocks that include the Unkar Group, the Nankoweap Formation, and the Chuar Group, display total thicknesses of about two miles, mostly of shale and limestone (Austin 1994). Even more impressive, the Mesoproterozoic (Precambrian) Belt Supergroup, exposed in western Montana, Idaho, Wyoming, Washington, and British Columbia, is mostly mudstone (shale, fine sand, and carbonate) and up to 8 miles in thickness (Winston and Link 1993). These examples hint that there may have been a vast quantity of mudrocks on the pre-Flood earth, possibly enough to account for most of the clay and carbonate rocks in the Flood sediment record. Exploring the consequences of initial conditions that include a substantial layer of pre-Flood mudstone sediments is an attractive task for future application of this model.

Appendix E of Baumgardner (2016) provides a description of the cavitation submodel. It is implemented in the numerical code by means of a single equation involving three adjustable parameters. One of these parameters is the cavitation threshold velocity. For the calculation described in this paper, that threshold velocity is set to 15 m/s, below which no cavitation, and hence no erosion, occurs. Appendix E also describes the criteria for deposition and for erosion of already deposited sediment.

Given that the average thickness of Flood sediments on the continents today is about 2,000 m, it is not surprising that a numerical model capable of eroding, transporting, and depositing that much sediment will yield sediment thicknesses in some locations that significantly exceed that average value. In early tests it was found that the calculations become unstable unless some degree of isostatic compensation is allowed in locations where the sediment thicknesses become large. Appendix F in Baumgardner (2016) describes how isostatic compensation is included. Symmetrical compensation is applied for the negative loads that arise from bedrock erosion.

To describe the water flow over the earth in a quantitative way, the numerical model makes use of what is known as the shallow water approximation. This approximation requires that the water depth everywhere be small compared with the horizontal scales of interest. The depth of the ocean basins today—and presumably also during the Flood—is about four kilometers. By contrast, the horizontal grid point spacing of the computation grid for the case described in this paper is about 120 km. The expected water depths over the continental regions, where our main interest lies, are yet much smaller than those of the ocean basins. Hence the shallow water approximation is entirely appropriate for this problem. That approximation allows the water flow over the surface of the globe to be described in terms of a single layer of water with laterally varying thickness. What otherwise would be an expensive three-dimensional problem now becomes a much more tractable two-dimensional one.

Appendix G in Baumgardner (2016) outlines the mathematical approach for solving the shallow water equations for the water velocity and water height over the surface of the earth as a function of time. These equations express the conservation of mass and the conservation of linear momentum. They are solved in a discrete manner using what is known as a semi-Lagrangian approach on a mesh constructed from the regular icosahedron as shown in Figure 1 of Baumgardner (2016).

A separate spherical coordinate system is defined at each grid point in that mesh such that the equator of the coordinate system passes through the grid point and the local longitude and latitude axes are aligned with the global east and north directions. The semi-Lagrangian approach, because of its low levels of numerical diffusion (Staniforth and Cote 1991), is also used for horizontal sediment transport. Seven layers of fixed thickness are used to resolve the sediment concentration in the vertical direction, with thinner layers at the bottom and thicker layers at the top of the column. These same numerical methods have been applied and validated in one of the world's foremost numerical weather forecast models, a model known as GME developed by the German Weather Service in the late 1990's (Majewski et al. 2002). The code that incorporates these many numerical features specifically for modeling the hydrological aspects of the Genesis Flood has been named 'Mabbul'. That word, of course, is the one used exclusively for the Flood in the Hebrew Old Testament.

2. Accounting for continent motion history

The previous study (Baumgardner 2016) utilized static continents. The present study has added a displacement history for the various continental blocks spanning, in terms of geological nomenclature, the Paleozoic, Mesozoic, and Cenozoic eras, that is, the portion of the geological record formed during the Flood. While the reconstruction of continent motions since the early Mesozoic has relatively small uncertainty because of the abundance of constraints from the present-day ocean floor, the motions during the Paleozoic typically have much more uncertainty because of the lack of surviving Paleozoic seafloor.

The primary observational data for recovering the Paleozoic continent motions are from paleomagnetism. Magnetic minerals in igneous rocks, provided that the rocks have not been significantly reheated since they crystalized, can record the orientation of the earth's magnetic field when the rocks crystallized. By measuring the magnetic declination and inclination in suitable igneous rocks from many points through the geological record for a given continent, one can construct a paleolatitude history for the continent. This procedure unfortunately provides no information on paleolongitude. Paleomagnetic determinations were first undertaken in the late 1940's. By the early 1950's paleomagnetic 'polar wander paths' for Europe and North America were being published showing that both continents, relative to today's North

Pole, had seemingly migrated northward dramatically since the mid-Paleozoic—by many tens of degrees. At the time this created quite a stir in the earth science community. In the decade of the 1960's, these paleomagnetic determinations helped convince many in the community that plates and plate mobility are indeed genuine realities. In subsequent decades more detailed and comprehensive paleomagnetic studies continued to reveal that same large amount of northward motion of Europe and North America relative to today's North Pole. The current estimated amount of northward motion is about 110°. From these studies it has been possible to reconstruct the history of continental motion during the Paleozoic to a reasonable level of confidence despite the lack of strong longitude constraints.

Several authors have published continent motion histories that span the neo-Proterozoic to present. The work described in this paper utilizes the global paleogeography maps by Ronald Blakey, emeritus professor of geology at Northern Arizona University, as a guide to that history. (An animation is available at https://www.youtube.com/watch?v=GGtQ1zpsdx4.) Blakey's map for the Early Cambrian (540 Ma in terms of the secular time scale) provides important insight into the continent configuration at the onset of the Flood. That map can be accessed online at http://scienceviews.com/photo/medium/SIA3660.jpg. In terms of the Flood, this snapshot corresponds to shortly after the breakup of a pre-Flood supercontinent. Some, including this author, refer to that supercontinent as Pannotia, while others, including Blakey, refer to it as Rodinia. At this early stage in the cataclysm the continental blocks known as Laurentia (corresponding to North America and Greenland), Baltica (corresponding to modern Western Europe), and Siberia (corresponding to Eastern Europe) have only recently broken away from the rest of Pannotia in a northerly direction. Although it is nearly impossible to discern in this global projection, the large portion of Pannotia known as Gondwana, composed of modern South America, Africa, Madagascar, India, Australia, and Antarctica, remains intact throughout the Paleozoic era to become part of Pangea. The remaining portions of Pannotia includes blocks that later become modern China and other parts of modern Asia.

Three subsequent snapshots in time from Blakey's set of global paleogeography maps provide a representative picture of the continental motion during the Paleozoic era. The snapshot for the Late Ordovician (450 Ma in terms of the secular time frame) shows Laurentia, Baltica, and Siberia progressively moving away from the rest of Pannotia and from one another. (This map can be accessed online at http://scienceviews.com/photo/medium/SIA3663.jpg.) The next snapshot for the Early Devonian (400 Ma in terms of the secular time frame) shows Laurentia and Baltica then reversing directions relative to one another and colliding back together. (This map can be accessed at http://scienceviews.com/photo/medium/SIA3665.jpg.) The final snapshot for the Pennsylvanian, (300 Ma in terms of the secular time frame) shows the remainder of Pannotia moving northward in the eastern hemisphere, crossing the South Pole, and colliding with Laurentia/Baltica from the south and that assembly in turn colliding with Siberia, also from the south. (That map can be accessed at http://scienceviews.com/photo/medium/SIA3668.jpg.) This paper utilizes this basic dynamic paleogeography as its guide for specifying the motions of the continental blocks as a function of time during the Flood.

One can inquire as to the reliability of continent motion reconstructions such as Blakey's. My own assessment is that the basic features are robust. They are based on vast numbers of paleomagnetic determinations stretching back more than 60 years by many investigators from all the continents. They are also based on a vast amount of geological field observation, including indisputable evidence for continent-continent collisions during the Paleozoic and associated orogenies, including the Caledonian orogeny involving Europe and North America, the Variscan/Hercynian/Appalachian orogeny involving Europe, North America, and Africa, and the Uralian orogeny involving Europe and Asia/Siberia. While many of the details may remain uncertain, to me there is little reason to question the basic history of relative motions.

3. The issue of polar wander

One aspect of the picture that to me is subject to question is the issue of whether the large changes in paleomagnetic latitude are to be interpreted as apparent polar wander or possibly instead as true polar wander. Interpreting them as apparent polar wander implies that the magnetic poles have remained largely fixed and the continents have moved vast distances. Allowing for a significant amount of true polar wander allows for the continents to have moved dramatically shorter distances over the earth's surface—distances that can readily be accounted for by normal plate tectonics. This issue is exacerbated as one considers the brief time span of the Flood. It is incredibly difficult to conceive of a mechanism by which the huge Gondwanan continent might move around the earth by more than a quarter of the earth's circumference in such a short interval of time. While it is not that obvious as to how that amount of true polar wander might have occurred in such a brief time window, the processes of transport of a large volume of cold lithosphere from the earth's surface into the deeper mantle and the rising of a comparable volume of hot mantle rock from the core/mantle boundary into the mid and upper mantle may have temporarily altered the earth's rotational moments of inertia sufficiently to produce the wander within the time span of the Flood. This is a topic to be explored in future studies.

Based on these considerations the choice was made to assume that 110° of true polar wander of the earth's spin axis occurred during the Flood, most of it during its earlier stages. It was found appropriate to assume that the plane in which the polar wander occurred was the defined approximately by today's 0° or prime meridian that runs through Greenwich, England. With these assumptions it becomes possible to rotate Pannotia 110° clockwise, when viewed from the east, on the computational grid such that Africa in Pannotia coincides with Africa today in its location on the earth. To account properly for the Coriolis effect, one simply alters the orientation of the spin axis appropriately with respect to the computational grid, involving merely a trivial change in the coding. The actual true polar wander is accounted for by allowing the orientation of the spin axis to change with time in a specified way. This approach allows for all the motion of the continental blocks to be actual plate motion. Moreover, it becomes dramatically simpler to compare Pannotia with Pangea directly from the plots. One discovers that, apart from the terranes that form Asia today,

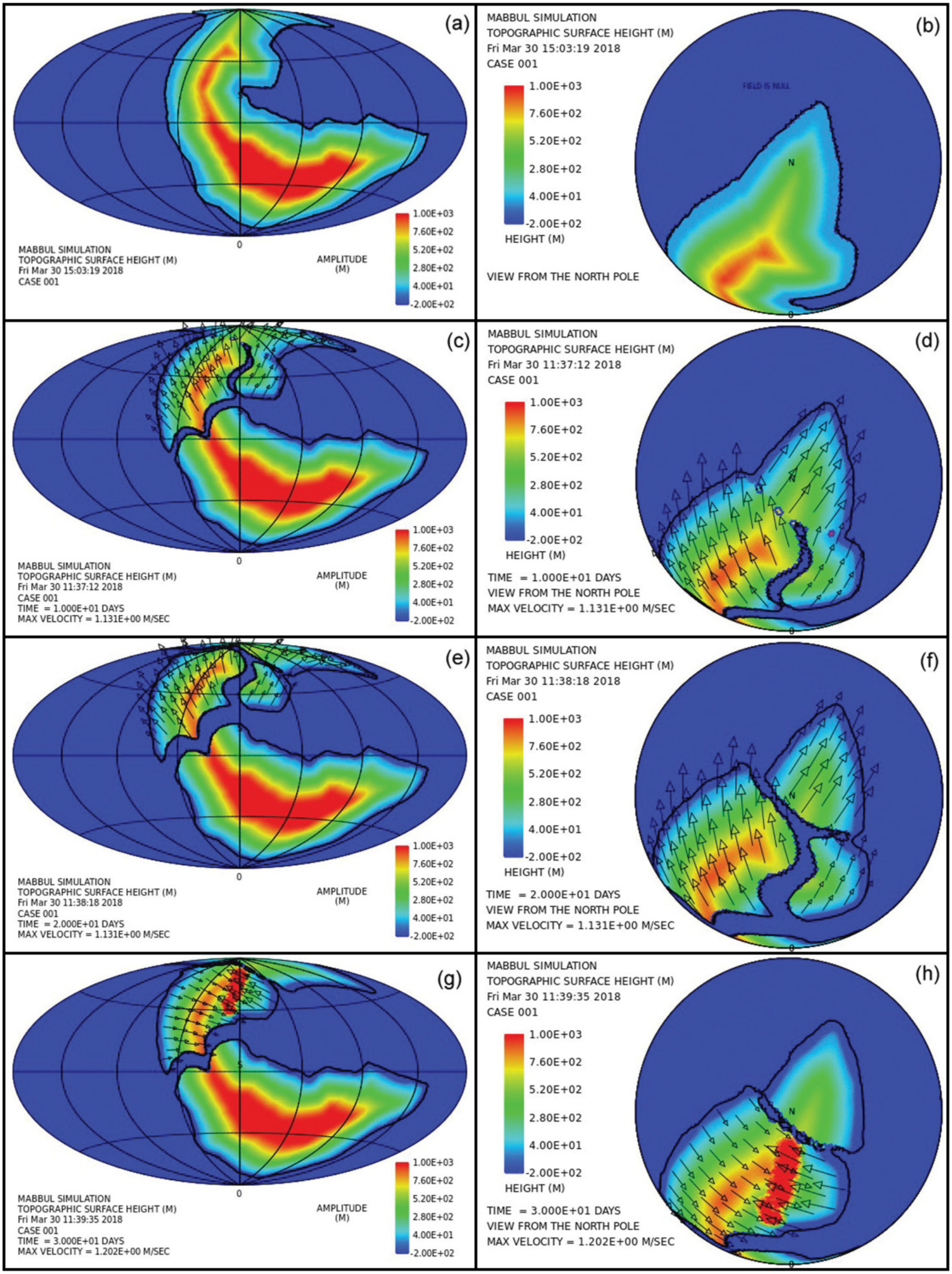
(a)
MABBUL SIMULATION
TOPOGRAPHIC SURFACE HEIGHT (M)
Fri Mar 30 15:03:19 2018
CASE 001
AMPLITUDE (M)
1.00E+03
7.60E+02
5.20E+02
2.80E+02
4.00E+01
-2.00E+02
0
(b)
MABBUL SIMULATION
TOPOGRAPHIC SURFACE HEIGHT (M)
Fri Mar 30 15:03:19 2018
CASE 001
HEIGHT (M)
VIEW FROM THE NORTH POLE
FIELD IS NULL
N
(c)
MABBUL SIMULATION
TOPOGRAPHIC SURFACE HEIGHT (M)
Fri Mar 30 11:37:12 2018
CASE 001
TIME = 1.000E+01 DAYS
MAX VELOCITY = 1.131E+00 M/SEC
(d)
MABBUL SIMULATION
TOPOGRAPHIC SURFACE HEIGHT (M)
Fri Mar 30 11:37:12 2018
CASE 001
TIME = 1.000E+01 DAYS
VIEW FROM THE NORTH POLE
MAX VELOCITY = 1.131E+00 M/SEC
(e)
MABBUL SIMULATION
TOPOGRAPHIC SURFACE HEIGHT (M)
Fri Mar 30 11:38:18 2018
CASE 001
TIME = 2.000E+01 DAYS
MAX VELOCITY = 1.131E+00 M/SEC
(f)
MABBUL SIMULATION
TOPOGRAPHIC SURFACE HEIGHT (M)
Fri Mar 30 11:38:18 2018
CASE 001
TIME = 2.000E+01 DAYS
VIEW FROM THE NORTH POLE
MAX VELOCITY = 1.131E+00 M/SEC
(g)
MABBUL SIMULATION
TOPOGRAPHIC SURFACE HEIGHT (M)
Fri Mar 30 11:39:35 2018
CASE 001
TIME = 3.000E+01 DAYS
MAX VELOCITY = 1.202E+00 M/SEC
(h)
MABBUL SIMULATION
TOPOGRAPHIC SURFACE HEIGHT (M)
Fri Mar 30 11:39:35 2018
CASE 001
TIME = 3.000E+01 DAYS
VIEW FROM THE NORTH POLE
MAX VELOCITY = 1.202E+00 M/SEC

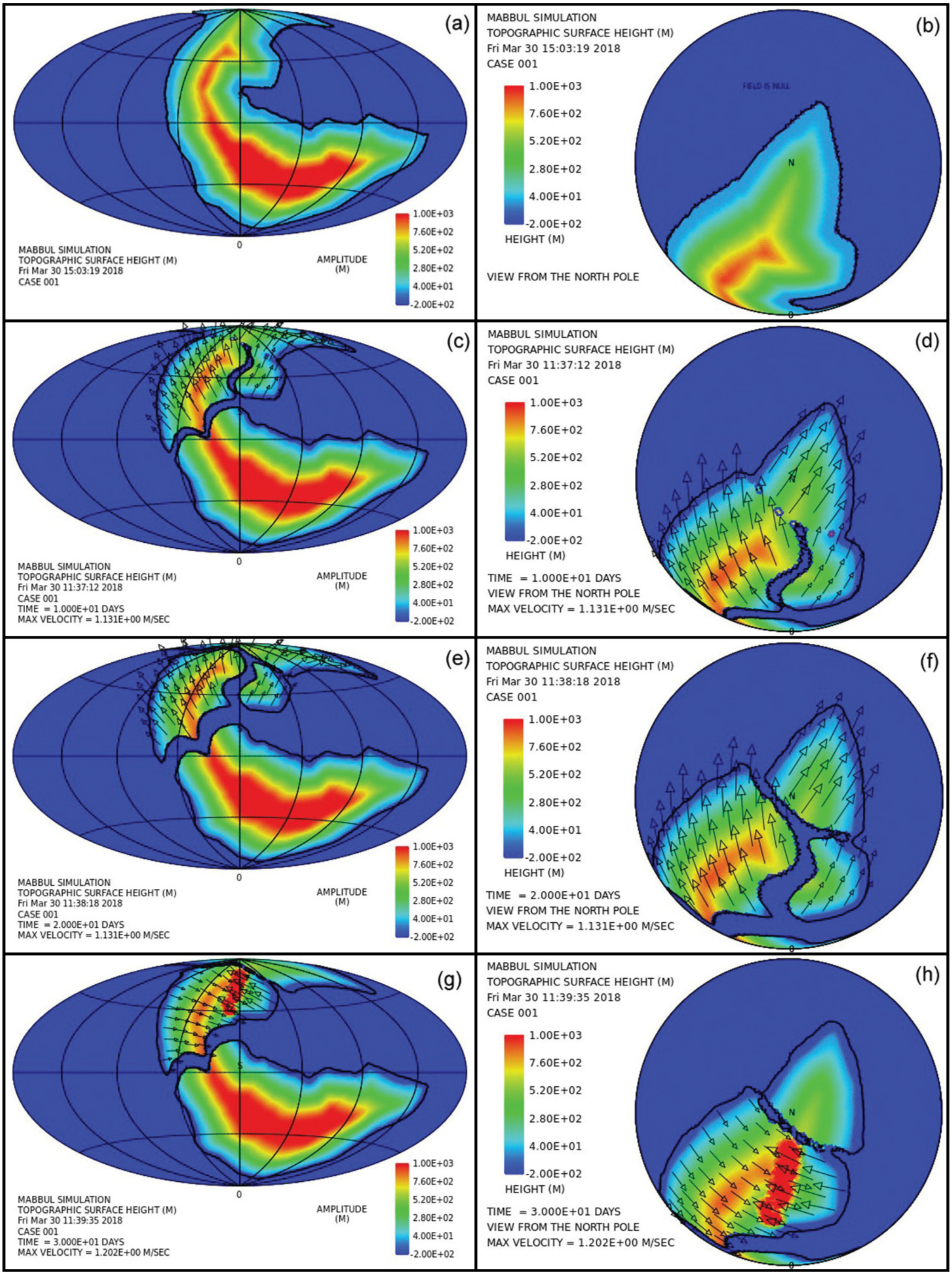
(a)
MABBUL SIMULATION
TOPOGRAPHIC SURFACE HEIGHT (M)
Fri Mar 30 15:03:19 2018
CASE 001
AMPLITUDE (M)
1.00E+03
7.60E+02
5.20E+02
2.80E+02
4.00E+01
-2.00E+02
(b)
MABBUL SIMULATION
TOPOGRAPHIC SURFACE HEIGHT (M)
Fri Mar 30 15:03:19 2018
CASE 001
HEIGHT (M)
VIEW FROM THE NORTH POLE
FIELD IS NULL
(c)
MABBUL SIMULATION
TOPOGRAPHIC SURFACE HEIGHT (M)
Fri Mar 30 11:37:12 2018
CASE 001
TIME = 1.000E+01 DAYS
MAX VELOCITY = 1.131E+00 M/SEC
(d)
MABBUL SIMULATION
TOPOGRAPHIC SURFACE HEIGHT (M)
Fri Mar 30 11:37:12 2018
CASE 001
TIME = 1.000E+01 DAYS
VIEW FROM THE NORTH POLE
MAX VELOCITY = 1.131E+00 M/SEC
(e)
MABBUL SIMULATION
TOPOGRAPHIC SURFACE HEIGHT (M)
Fri Mar 30 11:38:18 2018
CASE 001
TIME = 2.000E+01 DAYS
MAX VELOCITY = 1.131E+00 M/SEC
(f)
MABBUL SIMULATION
TOPOGRAPHIC SURFACE HEIGHT (M)
Fri Mar 30 11:38:18 2018
CASE 001
TIME = 2.000E+01 DAYS
VIEW FROM THE NORTH POLE
MAX VELOCITY = 1.131E+00 M/SEC
(g)
MABBUL SIMULATION
TOPOGRAPHIC SURFACE HEIGHT (M)
Fri Mar 30 11:39:35 2018
CASE 001
TIME = 3.000E+01 DAYS
MAX VELOCITY = 1.202E+00 M/SEC
(h)
MABBUL SIMULATION
TOPOGRAPHIC SURFACE HEIGHT (M)
Fri Mar 30 11:39:35 2018
CASE 001
TIME = 3.000E+01 DAYS
VIEW FROM THE NORTH POLE
MAX VELOCITY = 1.202E+00 M/SEC

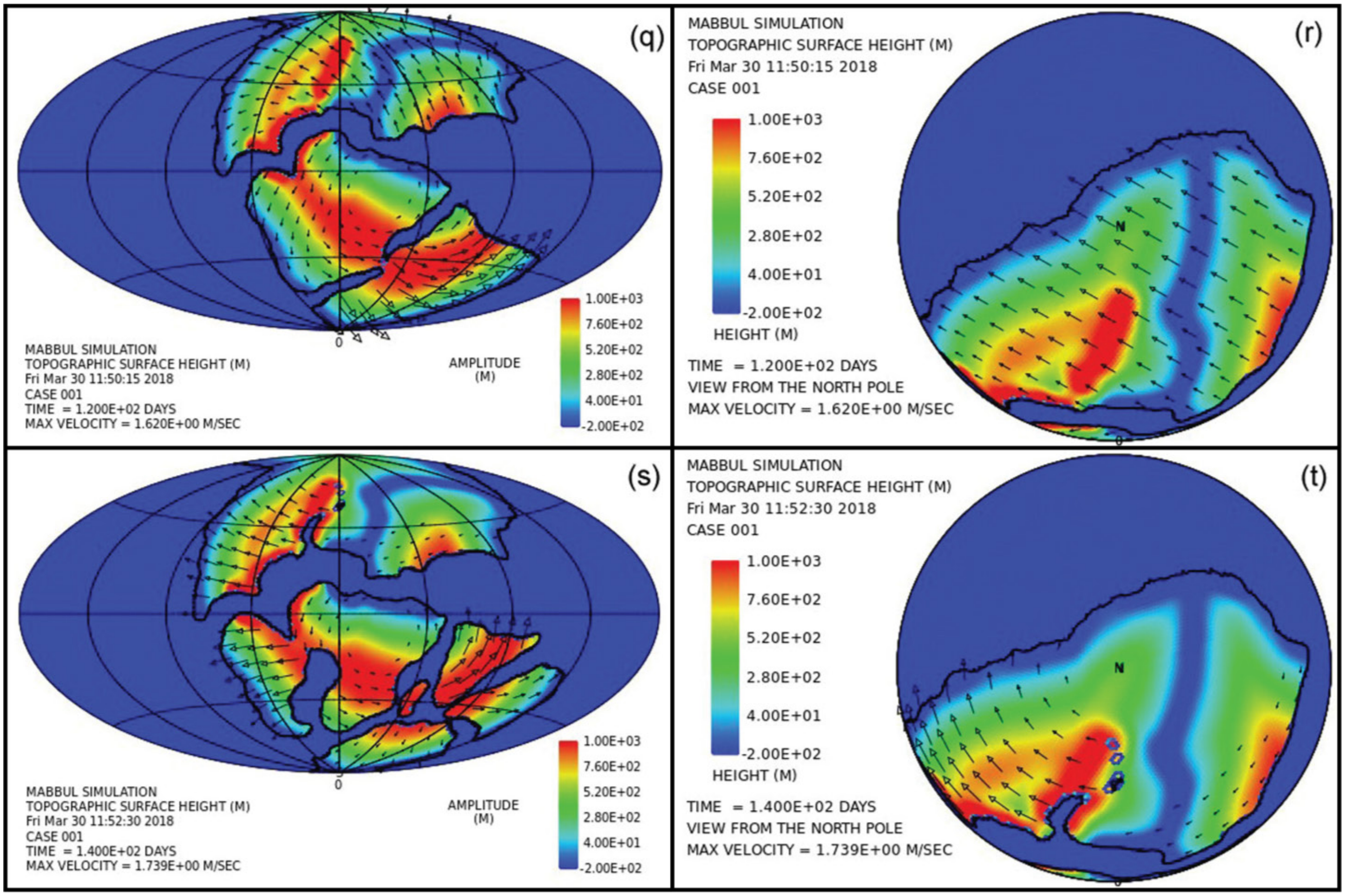

Figure 1 (begins on preceding pages). Snapshots in equal-area projection and geographic North Pole orthographic projection from the continent motion history assumed in this model at times of 0 days **(a)**, **(b)**; 10 days **(c)**, **(d)**; 20 days **(e)**, **(f)**; 30 days **(g)**, **(h)**; 40 days **(i)**, **(j)**; 50 days **(k)**, **(l)**; 90 days **(m)**, **(n)**; 110 days **(o)**, **(p)**; 120 days **(q)**, **(r)**; and 140 days **(s)**, **(t)**. Arrows indicate the instantaneous lateral velocities of the individual blocks. Colors indicate topographic height relative to mean sea level. The localized regions of elevated topography represent mountain belts resulting from collisions between Laurentia and Baltica (Caledonian orogeny) and between Laurentia and Africa (Variscan/Hercynian/Appalachian orogeny). Blue regions beyond the dark contour lines marking the continental boundaries correspond to deep ocean with a uniform depth of 4,000 m below mean sea level. The blue stripe that straddles the boundary between Siberia/Baltica and Asia in **(m)-(t)** is a consequence of the assumed initial low coastal topography of Pannotia. Note that this sequence of plots shows only the assumed continental motions. Tsunami activity is turned off, and there is no water movement.

the two supercontinents are remarkably similar. That should not be surprising because the entirety of Gondwana did not change between the two supercontinent configurations, and the blocks of Laurentia, Baltica, and Siberia changed relatively little.

4. Including continent motion history in the numerical model

To include the continent motion histories within the numerical framework required that a representation of the motion of each continent block as a function of time be incorporated. This was accomplished by specifying rotation poles for each of 11 different continental blocks and each of 10 separate time intervals. Each rotation pole is a vector in space with three components (x, y, z) that specifies the rate of displacement of the rigid block over the surface of the sphere during the time interval. As might be surmised, obtaining those rotation poles guided by the paleogeographic maps was a moderately tedious process. Figure 1 (a)-(t) provides snapshots from the resulting time history. Arrows indicate the motions of the individual blocks. Colors indicate topographic height relative to mean sea level. Blue regions beyond the dark contour lines marking the continental boundaries correspond to deep ocean. The continental configuration depicted in Figure 1 (a) and (b) is intended to represent the configuration that existed at the onset of the Flood, namely, that of Pannotia as mentioned earlier. The continent configuration depicted in Figure 1 (m) and (n) represents the configuration at the end of the Paleozoic generally referred to as Pangea. The primary difference between Pannotia and Pangea in this model is the location of the land area that today corresponds to eastern Asia. In Pannotia this land area adjoins Gondwana along its northeastern boundary. In secular continent motion histories this land area is also similarly adjoined to Gondwana, but splits away in multiple, successive slices that migrate northward and coalesce to become eastern Asia. In this numerical treatment the complexity of the multiple slices is omitted, and that entire region is treated instead as a single block. By removing what this author is convinced is true polar wander, Pannotia and Pangea, apart from eastern Asia, plot almost on top of one another. Their striking similarity thereby becomes much easier

to visualize and understand. Moreover, it requires dramatically less plate motion and less ocean floor subduction for Pannotia to be transformed into Pangea than do the secular reconstructions.

RESULTS

We shall now present results from a case with the water motion driven by large-amplitude tsunamis that includes the continent motion history just described. As mentioned in the introduction, these tsunamis are understood to be generated in subduction zones as the overriding plate—after an interval of being locked against a subducting plate—suddenly unlocks, and the two plates rapidly slip past each other. While the two plates are locked together, the sea bottom is dragged downward by the steadily sinking lithospheric slab beneath. When the plates unlock, the sea bottom rapidly rebounds, generating a large-amplitude tsunami. For the case shown in this paper, zones of subduction are chosen to lie along great circle arcs. These zones are divided into sixteen distinct segments, each about 14° of arc in length, which is about 1,500 km. Subduction is assumed to be occurring at an angle of 45° into the mantle along each of these segments with the horizontal speed of the subducting plate assumed to be 1.6 m/s at the beginning of the calculation, increasing to 1.9 m/s at 30 days, and to 2.0 m/s at 70 days.

While the subducting and overriding plates are locked, the seafloor in the subduction zone is assumed to be moving vertically downward at a rate of 0.707 times the assumed horizontal plate velocity because of the steady sinking motion of the subducting lithospheric slab beneath. Every two computational time steps, corresponding to an interval 360 s or 6 minutes, one of the 16 segments is allowed to unlock and slip, allowing the bottom of the subduction zone trench to rebound to its nominal, undepressed height. An individual segment therefore slips every 96 minutes. The amplitude of the rebound of the trench bottom is between 6,520 m and 8,140 m (1.6-2.0 m/s x 0.707 x 96 x 60 s). This impulsive uplift of the approximately 14° segment of trench bottom initiates a tsunami that travels across the 4,000-m deep ocean at a speed of about 200 m/s. The generation rate of one tsunami every six minutes is equivalent to 240 per day and 36,000 over a time span of 150 days. Initially the water is assumed to be at rest with its surface at sea level. The continent surface is assumed everywhere to consist of crystalline bedrock. The earth is assumed to be spinning at its current rate of rotation.

Understanding the results from the model is a challenge because of the model's many variable quantities such as water velocity, water depth, erosion rate, cumulative erosion depth, suspended sediment according to particle size for multiple particle size classes, deposited sediment according to particle size, and topographic height accounting for erosion, sedimentation, and isostatic adjustment, just to name a few. Each of these quantities varies both in time and potentially with respect to some 40,000 grid points that span the earth's surface. The only way a human being can possibly interact with such vast amounts of numerical information is for the information to be represented in a visual manner and then sampled only sparsely in time. Space restrictions in a written paper impose additional limitations.

With these considerations in view, I have chosen to include a relatively small set of color plots at a few points in time from the calculation to attempt to afford the reader the opportunity for at least a qualitative grasp of the model results. The times I have selected are at 20, 50, 80, 110, and 140 days from the start of the simulation. Because the continent motion history in this model is similar to that derived from some 70 years of study by the secular geology and geophysics communities, it is possible to connect times in this model with corresponding points in the standard geological time scale. The continent configuration at 20 days corresponds to 470 million years ago in the standard geological time scale (early Ordovician), 50 days to 320 million years ago (early Pennsylvanian/ mid-Carboniferous), 80 days 220 million years ago (late Triassic), 110 days to 160 million years ago (late Jurassic), and 140 days to 40 million years ago (mid-to-late Eocene).

Figure 2 provides plots at 20 days for the surface height of either the water or land, whichever is greater; the water depth over the land surface, the cumulative depth of bedrock erosion, the amount of suspended sediment (all particle sizes combined), and the net cumulative depth of deposited sediment. Plots (a) and (b) clearly show water waves in the deep ocean with trough to crest amplitudes of more than 2,000 m. These waves correspond to the tsunamis generated in a repetitive manner, every 96 minutes at a given location, along active subduction zones. Such waves propagate at a speed of 200 m/s in the deep ocean. Plots (c) and (d) of water depth show the extent of the invasion of the tsunami waves onto the land surface. Generally speaking, it is the lower elevation coastal regions that have been flooded at this stage in the simulation. Plots (e) and (f) display the cumulative depth of crystalline bedrock erosion. As might be expected, the most intense erosion is occurring along the continent margins where the tsunami waves encounter the abrupt topographic change from deep ocean to continent. Plots (g) and (h) display the total amount of suspended sediment for all particle sizes, in terms of solid equivalent, in the turbulent water column. Coarse particles tend to settle out of suspension more quickly and nearer to where they have generated by cavitation compared with the finer ones. Plots (i) and (j) show the cumulative amount of sediment deposition of all sediment sizes. Regions of thick deposition generally occur in a band just inland from the coast. It is noteworthy that already at this stage in the simulation these zones in the coastal lowlands display sediment thicknesses of more than 350 m. At 20 days the average depth of bedrock erosion over the entire continent surface is 143 m. The average depth of sediment accumulation is 140 m, and the average amount of sediment in suspension is 3 m, where the averages are over the continental surface area. In all these plots the displacements of Laurentia, Baltica, and Siberia away from the remainder of Pannotia are evident.

Figure 3 provides plots at 50 days of water/land surface height, water depth over the land surface, cumulative depth of bedrock erosion, net cumulative depth of deposited sediment. By this stage in the calculation, Baltica and Laurentia have reversed direction and collided with each other, resulting in the Caledonian orogeny. That block has in turn collided with Gondwana, producing the Variscan/ Hercynian/ Appalachian orogeny. Siberia has also collided with Baltica and Laurentia such that Siberia, Baltica, Laurentia, and Gondwana are now all joined together in a manner very similar to

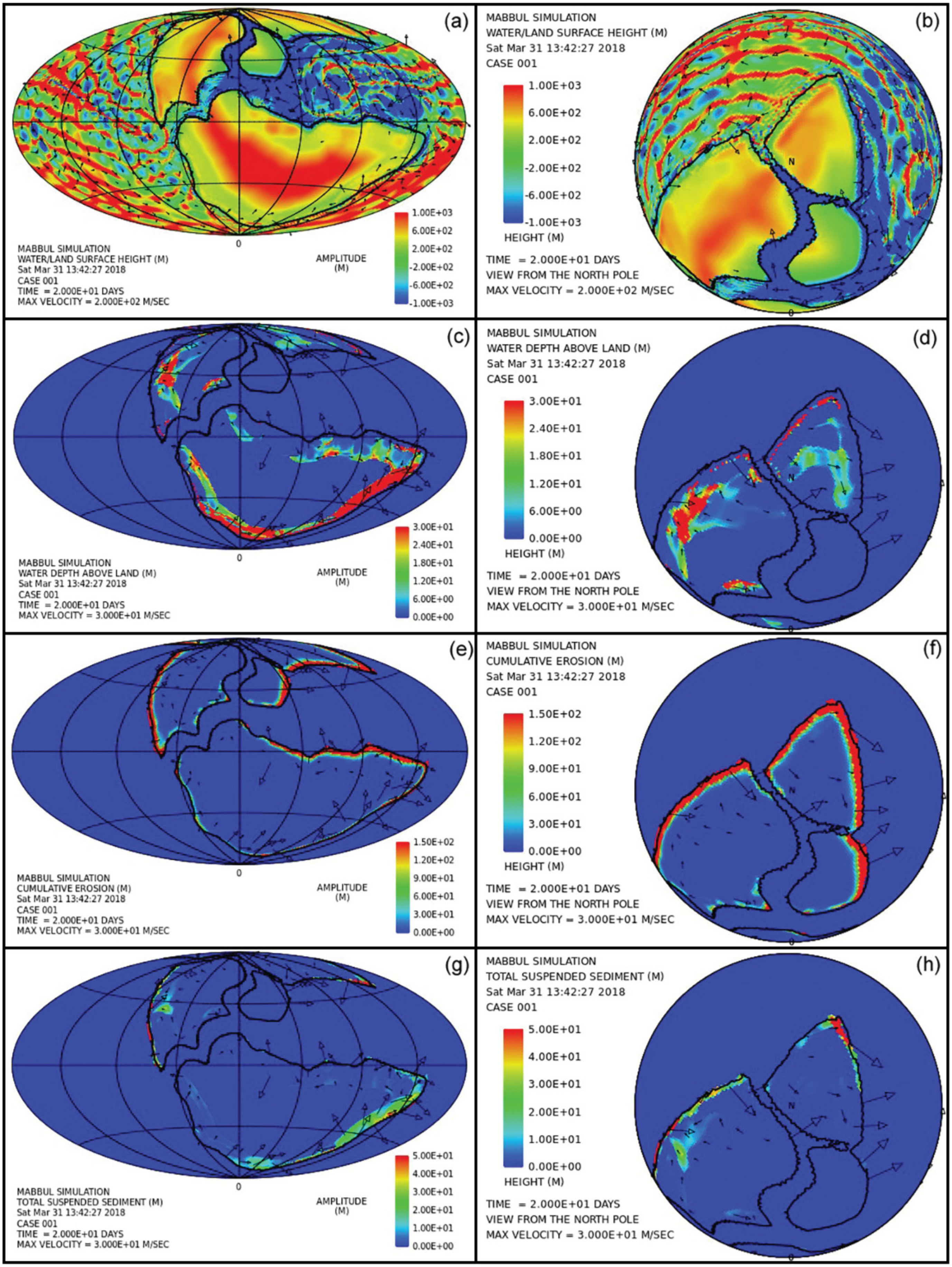
(a)
MABBUL SIMULATION
WATER/LAND SURFACE HEIGHT (M)
Sat Mar 31 13:42:27 2018
CASE 001
TIME = 2.000E+01 DAYS
MAX VELOCITY = 2.000E+02 M/SEC
AMPLITUDE (M)
1.00E+03
6.00E+02
2.00E+02
-2.00E+02
-6.00E+02
-1.00E+03
(b)
MABBUL SIMULATION
WATER/LAND SURFACE HEIGHT (M)
Sat Mar 31 13:42:27 2018
CASE 001
1.00E+03
6.00E+02
2.00E+02
-2.00E+02
-6.00E+02
-1.00E+03
HEIGHT (M)
TIME = 2.000E+01 DAYS
VIEW FROM THE NORTH POLE
MAX VELOCITY = 2.000E+02 M/SEC
(c)
MABBUL SIMULATION
WATER DEPTH ABOVE LAND (M)
Sat Mar 31 13:42:27 2018
CASE 001
TIME = 2.000E+01 DAYS
MAX VELOCITY = 3.000E+01 M/SEC
AMPLITUDE (M)
3.00E+01
2.40E+01
1.80E+01
1.20E+01
6.00E+00
0.00E+00
(d)
MABBUL SIMULATION
WATER DEPTH ABOVE LAND (M)
Sat Mar 31 13:42:27 2018
CASE 001
3.00E+01
2.40E+01
1.80E+01
1.20E+01
6.00E+00
0.00E+00
HEIGHT (M)
TIME = 2.000E+01 DAYS
VIEW FROM THE NORTH POLE
MAX VELOCITY = 3.000E+01 M/SEC
(e)
MABBUL SIMULATION
CUMULATIVE EROSION (M)
Sat Mar 31 13:42:27 2018
CASE 001
TIME = 2.000E+01 DAYS
MAX VELOCITY = 3.000E+01 M/SEC
AMPLITUDE (M)
1.50E+02
1.20E+02
9.00E+01
6.00E+01
3.00E+01
0.00E+00
(f)
MABBUL SIMULATION
CUMULATIVE EROSION (M)
Sat Mar 31 13:42:27 2018
CASE 001
1.50E+02
1.20E+02
9.00E+01
6.00E+01
3.00E+01
0.00E+00
HEIGHT (M)
TIME = 2.000E+01 DAYS
VIEW FROM THE NORTH POLE
MAX VELOCITY = 3.000E+01 M/SEC
(g)
MABBUL SIMULATION
TOTAL SUSPENDED SEDIMENT (M)
Sat Mar 31 13:42:27 2018
CASE 001
TIME = 2.000E+01 DAYS
MAX VELOCITY = 3.000E+01 M/SEC
AMPLITUDE (M)
5.00E+01
4.00E+01
3.00E+01
2.00E+01
1.00E+01
0.00E+00
(h)
MABBUL SIMULATION
TOTAL SUSPENDED SEDIMENT (M)
Sat Mar 31 13:42:27 2018
CASE 001
5.00E+01
4.00E+01
3.00E+01
2.00E+01
1.00E+01
0.00E+00
HEIGHT (M)
TIME = 2.000E+01 DAYS
VIEW FROM THE NORTH POLE
MAX VELOCITY = 3.000E+01 M/SEC

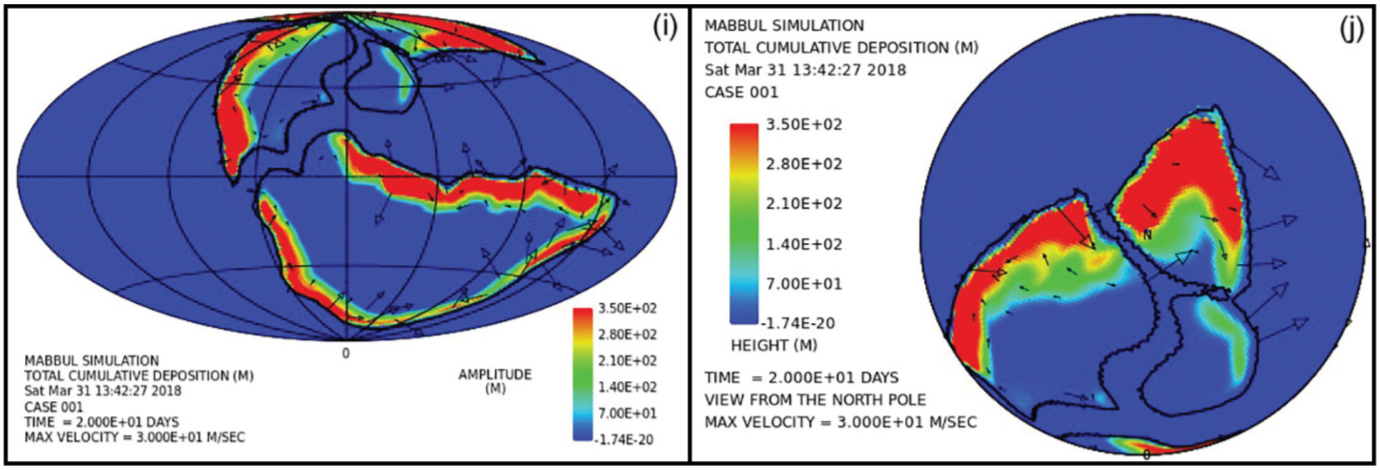

Figure 2 (begins of preceding page). Plots in equal-area projection and geographic North Pole orthographic projection at 20 days of water or land surface height, whichever is greater, **(a)**, **(b)**; water depth over the land surface, **(c)**, **(d)**; cumulative depth of bedrock erosion, **(e)**, **(f)**; suspended sediment (all particle sizes combined), **(g)**, **(h)**; and cumulative depth of deposited sediment, **(i)**, **(j)**. In **(a)** and **(b)** arrows denote water column velocities, clipped at 200 m/s. In **(c)-(h)** arrows denote water velocities just above the land surface, clipped at 30 m/s.

their earlier locations in Pannotia. Notably, the portion of continent that is to become eastern Asia has broken away from what earlier had been northeastern Pannotia and is now moving northward. At this point in the calculation the south rotational pole has moved to approximately 48° south latitude (marked by S on the equal area plots) along the zero-longitude meridian. A large gyre whose center is near the north rotational pole is prominent in plots (a) and (b) above deep ocean on the opposite side of the earth. Plots (i) and (j) show that sediment continues to accumulate in the zones adjacent to the coasts and that the zones are tending to expand inland. At 50 days the average depth of bedrock erosion over the entire continent surface is 442 m. The average depth of sediment accumulation is 435 m, and the average amount of sediment in suspension is 7 m.

Figure 4 displays the water/land surface height, the water depth over the land surface, the cumulative depth of bedrock erosion, and the net cumulative depth of deposited sediment at a time of 80 days. At this stage in the calculation, the east Asia block is near to docking with the Siberian block. That docking, which occurs at 90 days, will complete the assembly of Pangea. At 80 days there are regions where sediment thickness has reached 1,500 m. On average there is 560 m of sediment over the land surface and 39 m of sediment in suspension.

Figure 5 displays, at a time of 110 days, water/land surface height, cumulative depth of bedrock erosion, and net cumulative depth of deposited sediment. At this point in the calculation, the Pangean supercontinent is beginning to break apart. The present North Atlantic Ocean is opening as northern portion of Pangea consisting of Laurentia and Eurasia rotates clockwise relative to Gondwana. The Gondwana block itself is beginning to rift apart along the eastern margin of what today is Africa. At this stage in the calculation the rotation axis matches today's orientation. The total volume of eroded sediment at this point is equal to an average of 901 m over the entirety of the continental surface.

Figure 6 displays the same fields at a time of 140 days. At this point Gondwana has disassembled into blocks corresponding to South America, Africa, Madagascar, India, Antarctica, and Australia, and Laurentia is beginning to split away from Eurasia in the north. The average amount of sediment deposited on the continent surface is now 1,162 m, and the average amount of sediment in suspension is 26 m.

DISCUSSION

1. Some challenges Flood models are called to explain

Serious intellectual defense of the Genesis Flood calls for substantive explanations for several major features of the earth's continental surface. First is the staggering ***volume*** of the fossil-bearing sedimentary rock present, corresponding to an average thickness of about 2,000 meters or about 1.2 miles. What was the source of such a massive quantity of sediment during such a brief span of time? Second is the ***location*** of this massive volume of sediment. It occurs *on top* of the continents, whose surface generally lies above sea level. What sort of water process might conceivably emplace so much sediment above sea level on top of that land surface? A third issue pertains to the ***vast horizontal extent*** of individual sediment layers with little to no erosional channeling between successive layers. This pattern is readily observed for the sediments exposed in the walls of the Grand Canyon. What sort of transport and depositional process could conceivably generate such uniform layers over such vast horizontal distances?

A fourth noteworthy issue is related to the third one. It is the presence of ***beds, separated by bedding planes***, on the scale of centimeters to meters which is such a prominent characteristic of sedimentary rocks. It is so common that it is almost taken for granted with little consideration of the processes responsible. It is as if the sediment is being deposited in pulses in a repeating manner, with each pulse producing a thin layer, commonly with vast horizontal extent as illustrated in Figure 7. Especially in the context of the Flood, what is the mechanism responsible for such repetitive and detailed structure?

A fifth prominent feature has to do with the manner in which these fossil-bearing sediment layers are organized into six massive packages known as ***megasequences*** that are separated from one another by what appear to be global-scale erosional unconformities. Again, in the context of the Flood, what mechanism might account for this pattern?

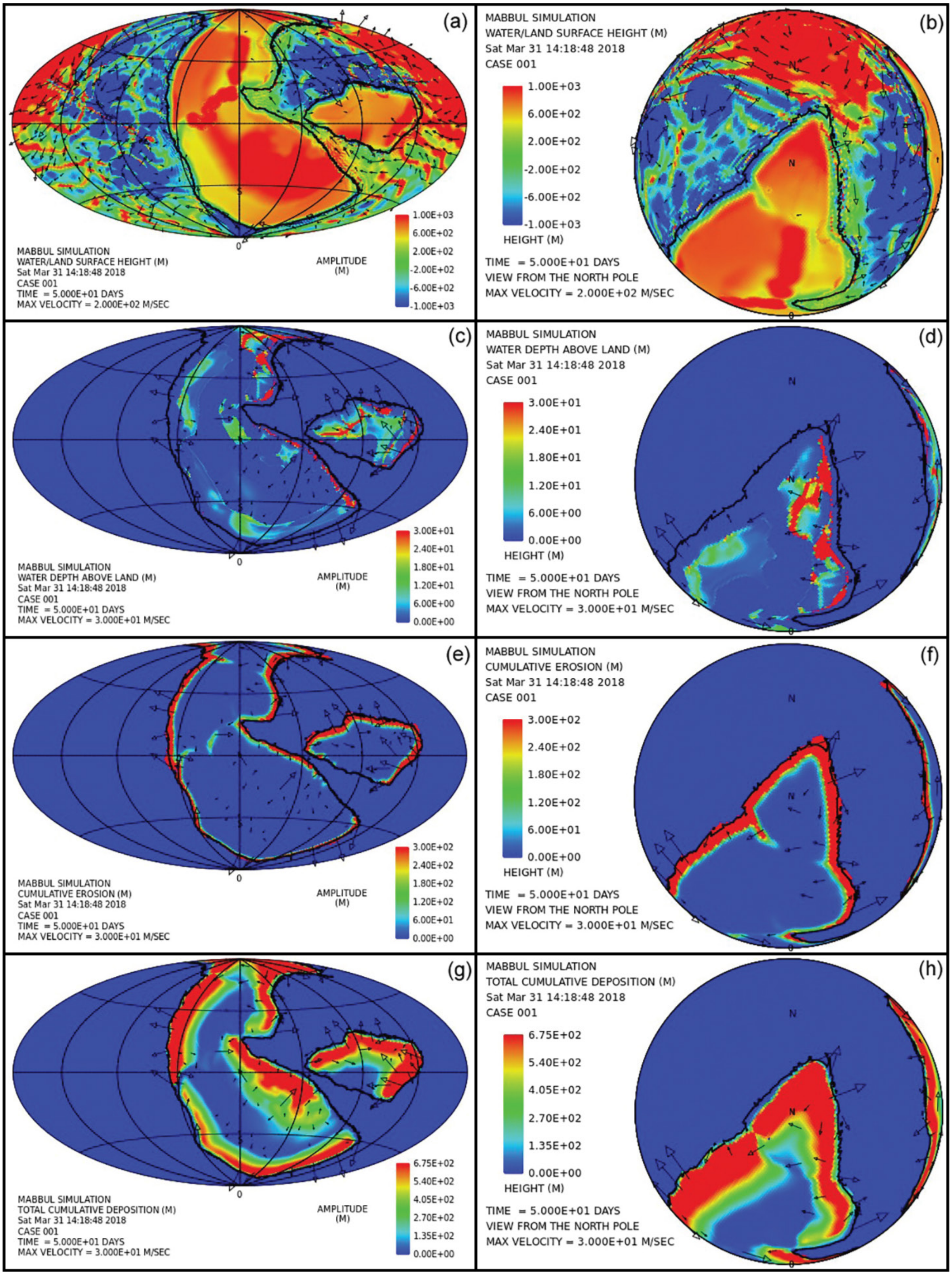

Figure 3. Plots at 50 days of water/land surface height **(a)**, **(b)**; water depth over the land surface, **(c)**, **(d)**; cumulative depth of bedrock erosion, **(e)**, **(f)**; and cumulative depth of deposited sediment, **(g)**, **(h)**. Arrows denote water velocities as in Figure 2.

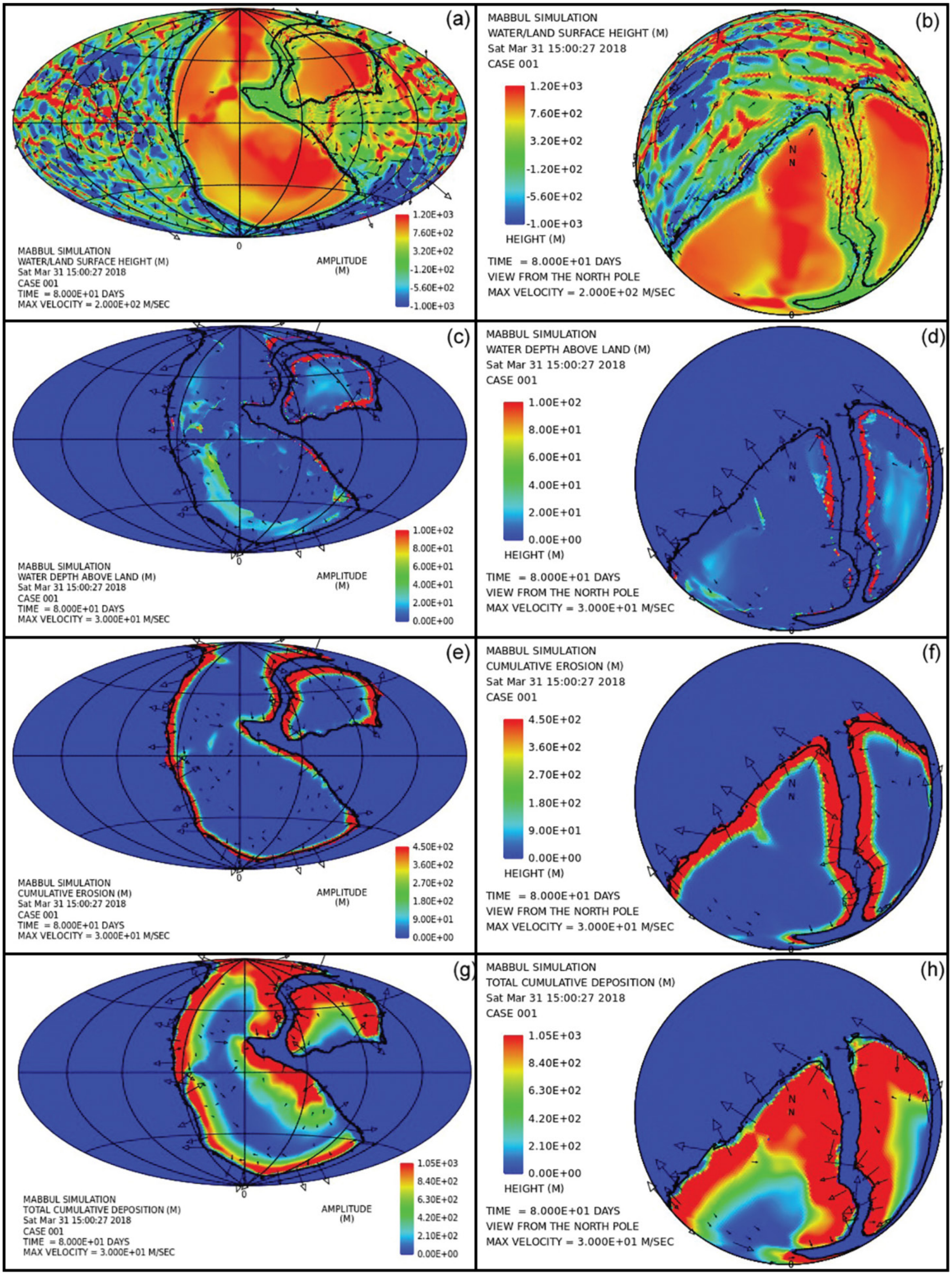

Figure 4. Plots at 80 days of water/land surface height **(a)**, **(b)**; water depth over the land surface, **(c)**, **(d)**; cumulative depth of bedrock erosion, **(e)**, **(f)**; and cumulative depth of deposited sediment, **(g)**, **(h)**.

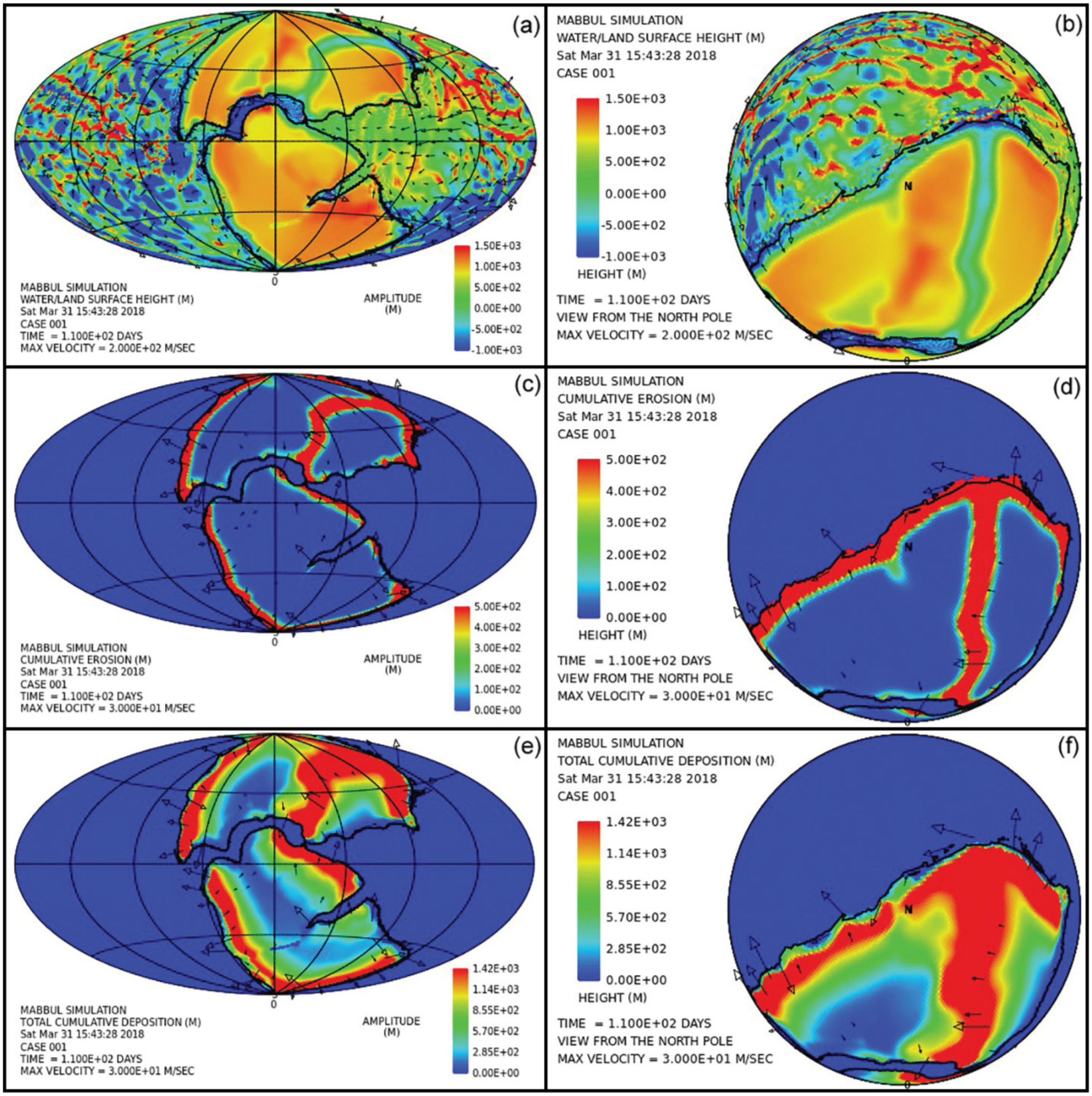

Figure 5. Plots at 110 days of water/land surface height **(a)**, **(b)**; cumulative depth of bedrock erosion, **(c)**, **(d)**; and cumulative depth of deposited sediment, **(e)**, **(f).**

A sixth notable aspect of the earth's surface geology are what are referred to as the ***continental shields***, including the Canadian, Baltic, Angaran (Siberian), African, Indian, Australian, and Antarctic shields. These large areas of exposed Precambrian crystalline igneous and high-grade metamorphic rocks have experienced significant erosion (often with more than 1 km of crystalline rock removed), are nearly flat, and have negligible, if any, sediment cover. When in earth history did such intense erosion occur if it was not during the Genesis Flood? And by what sort of process?

2. Encouraging new insights

The numerical investigation described in this paper shed important new light on most of these prominent issues. First, regarding a source for the huge volume of Phanerozoic sediment present in the continental rock record, the calculations reveal that tsunami-driven cavitation erosion during the time span of the Flood can generate new sediment at a rate sufficient to account for a sizable fraction of the Phanerozoic sediment inventory. The cavitation, occurring at water speeds of several tens of m/s, rapidly reduces crystalline continental crustal rock to sand-sized and smaller particles.

These sediment particles are readily suspended in the turbulent water associated with the tsunami as it makes its way at reduced horizontal speeds onto the continental surface. The large amplitudes of the tsunamis enable them readily to invade the

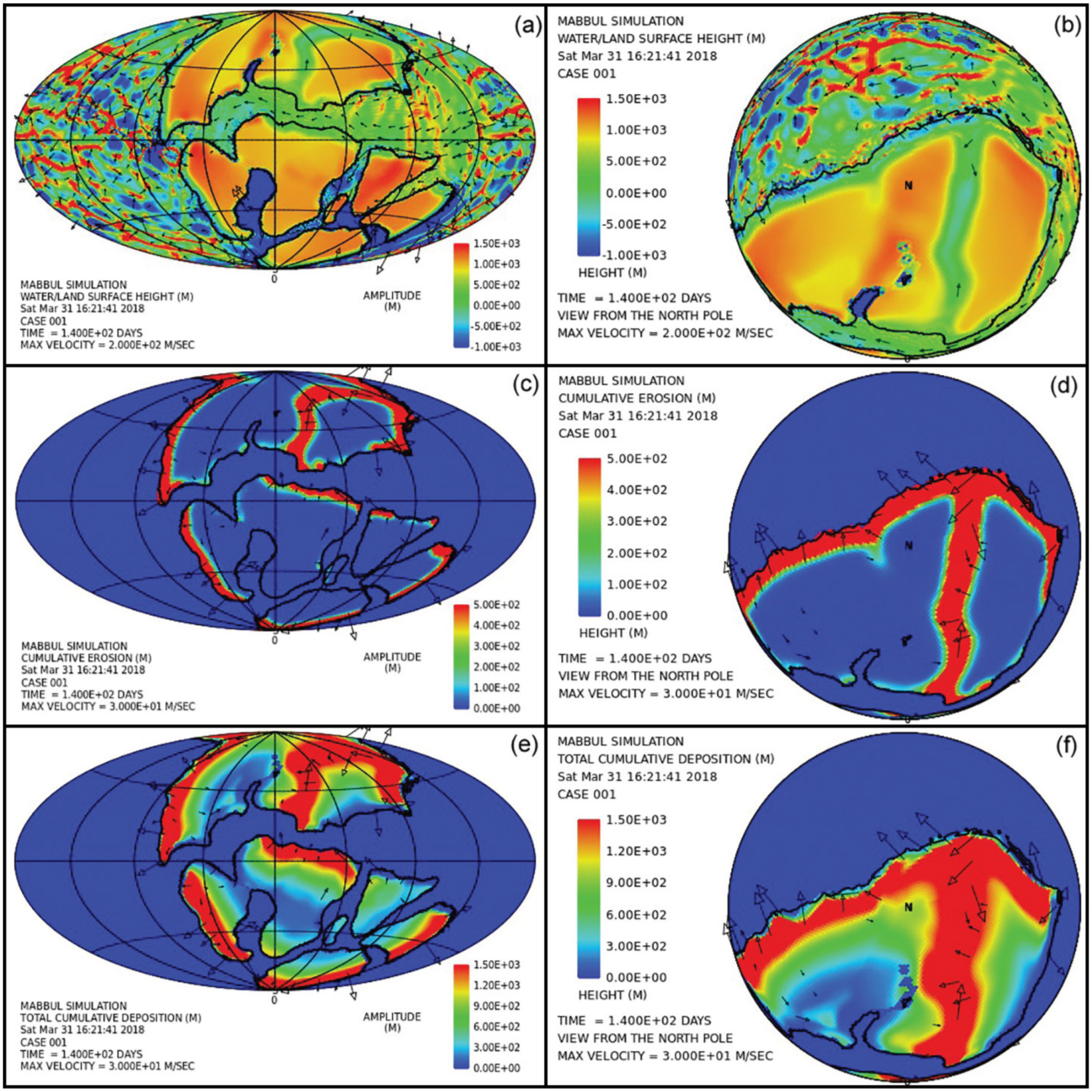

Figure 6. Plots at 140 days of water/land surface height **(a)**, **(b)**; cumulative depth of bedrock erosion, **(c)**, **(d)**; and cumulative depth of deposited sediment, **(e)**, **(f)**.

continent interiors with their load of suspended sediment. Details of the numerical results show that, just as there are ebb and flow phases of the tide on a beach, the tsunamis display similar back and forth flow. In a tide the *ebb* is the outgoing phase, when the tide drains away from the shore; the *flow* is the incoming phase when water rises again. In the case of the tsunamis, the incoming phase has much higher speed, is highly turbulent, keeps the sediment in suspension, and there is little or no deposition. By contrast, in the outgoing phase, the water speed is lower, the flow is less turbulent, and deposition typically is appreciable. In terms of the flow direction recorded in the deposited sediment implied by this model, the flow direction recorded in the deposited sediment is generally in the direction toward the coastline. For example, in the case of the Laurentia, which today corresponds to North America and Greenland, tsunamis in the model invade the western coast from the west southwest. The current direction of the retreating water from these tsunamis, when most of the sediment deposition occurs, is therefore from the east northeast. It is noteworthy that the paleocurrent directions observed in the Paleozoic portion of the sediment record in the southwestern United States are also predominately from the east northeast (Brand et al. 2015).

This framework also appears to explain a prominent feature of the sediment record largely ignored until now by Flood geologists, namely, the existence of *thousands* of individual beds separated by

Figure 7. Photo of a common characteristic of the sediment record, that of beds separated by bedding planes.

bedding planes in typical vertical sequences between continental basement and the earth's surface as illustrated in Figure 7. What conceivable mechanism could have produced such high frequency modulation of the sediment transport and deposition processes to yield so many distinct individual beds that commonly display huge lateral extent, yet with laterally uniform composition and character? The vast numbers of tsunamis that catastrophic plate tectonics appears to demand seems to be the answer. The length of each of the 16 subduction zone segments assumed in the model that locked and slipped every 96 minutes to generate a tsunami was 1,500 km. This produced a total of 36,000 tsunamis over the span of 150 days. But if we look at preset-day subduction zones for guidance, it is likely that the typical segment length was much shorter. Reducing the segment length to half of that assumed doubles the total number of mega-tsunamis to 72,000. Since these tsunamis are large enough to propagate at least once around the earth before their amplitude becomes small, they appear to provide a viable explanation for the modulated character observed in the vertical structure of the sediment record, especially at the bed level. In terms of the Flood and it brief time scale, it is difficult to imagine an alternative that could produce this high frequency modulation.

What insight might the calculation included in this paper provide as to the mechanism or mechanisms that may have been responsible for the megasequence structure of the fossil-bearing sediment record? The short answer is that this rather primitive calculation yields no hint of the sort of large scale pattern of transgression and recession of ocean water that seems to be implied by the megasequence morphology. The secular community generally interprets the megasequence structure to be the result of a variation in global sea level. Indeed, a rise and fall in sea level several times during the Flood, combined with the tsunami activity, does appear to offer a viable explanation. Other modeling work indicates that the rapid global tectonics and associated flow of rock inside the mantle during the Flood does lead to significant time-variation in global sea level (Baumgardner, 1994).

What about the issue of the continental shields? The existence so many shield areas today testifies to the reality of extreme erosion of the igneous bedrock over vast portions of today's continents. These shield areas are remarkably flat with little or no erosional channeling and generally display little or no sedimentary deposition subsequent to their intense erosional beveling. In the context of the Flood, these areas would seem to be obvious candidates as source areas for at least some of the sediment we find elsewhere on the continental surface. A major issue, however, is an erosional mechanism sufficiently potent to erode resistant crystalline bedrock to depths of up to a kilometer or more within the time span of the Flood and to do so in such a uniform manner across such laterally extensive areas. The frequent, large-amplitude tsunamis in this numerical model appear adequate for such a task. Indeed, it is difficult to imagine an alternative mechanism capable of accomplishing such intense and laterally extensive erosion to produce surfaces with such astonishing flatness.

In the calculation described in this paper it is noteworthy, however, that almost all the bedrock erosion occurs on the continental slope, with very little in the continental interior. One possible explanation is that the dynamic surface topography generated by stresses from flow of rock inside the mantle is not yet included in this formulation. Earlier calculations of the rapid tectonics during the Flood (e.g., Baumgardner 1994) reveal that deflections of the earth's surface by many kilometers arise from the flow of rock inside the mantle. When those dynamic up-and-down motions of the continent surfaces are included it is likely that significant bedrock erosion will indeed occur within the continent interiors. This issue merits priority in future numerical investigations.

Regarding an explanation for why so much sediment is emplaced on top of the continents when their surfaces mostly lie above sea level, these calculations provide especially helpful insight. The water speeds and depths are sufficient to sustain the level of turbulence needed to suspend the large volume rate of sediment produced by cavitational erosion, to transport it to distant locations, and to deposit that sediment on the continent surface in thicknesses exceeding more than a kilometer over vast areas. The tsunami-driven flow accounts not only for erosion of significant volumes of sediment but also its emplacement above sea level on top of the continents in coherent patterns with large horizontal dimensions and thicknesses. The model thus seems to account in a powerful way for the emplacement of the sediment on top of the continental surface in broad agreement with observations.

The tsunami mechanism also provides a trivially simple explanation for the runoff of the Flood water from the continental surface. As the gravitational potential energy from the sinking lithospheric slabs and rising mantle plumes which had been driving the runaway motions begin to be significantly depleted, the surface plate speeds diminish, the tsunamis decrease in frequency and amplitude, the flow rates of the water currents on the continents plummet, and the water that had repeatedly traversed the continental surface simply drains away, back into the ocean basins. The tsunami mechanism provides trivially simple answers to the commonly asked questions as to the source of the Flood waters and where these waters went after the Flood. The answers to both questions, of course, are the ocean basins.

3. Future model enhancements

It is important to emphasize that the numerical model described in this paper is highly simplified relative to the real earth and includes

only a subset of the processes in operation during the Flood. One noteworthy process not included pertains to sediment transport and deposition. Currently, sediment transport and deposition via the process of hyperconcentrated flow is missing. In the present treatment sediment falls out of suspension and deposits on the surface whenever the sediment carrying capacity in the turbulent water column is exceeded. It would be straightforward to utilize the bottommost two or three sublayers in the water column to handle the condition of hyperconcentrated flow when it happens to arise. It is anticipated that most of the deposition on the land surface would then occur when a developing hyperconcentrated flow becomes unstable as it switches from laminar to turbulent and dumps its sediment load. This enhancement should increase the realism of the model considerably.

Another process not currently included is the dynamic topography arising from flow of rock in the mantle. Variations in continent surface height from stresses produced by flow of rock in the mantle below can reach several kilometers in amplitude, especially in association with subduction near a continental margin (Baumgardner 1994). Such large amplitude dynamic topography must have affected the water flow and erosion/sedimentation patterns on the continents during the Flood in a major way. In addition, the time dependence of the tectonic processes responsible for the flow inside the mantle also affects the global sea level. Including some approximation of these dynamical processes may well account for the large-scale patterns of transgression and recession responsible for the megasequence structure of the overall sedimentary record.

Also missing is a realistic representation of initial topography of the pre-Flood continental surface beyond low topography adjacent to the coasts and higher topography in the continent interior. Recovering more realistic topographical features of Pannotia from clues in the Precambrian rocks will be a challenging endeavor. On the other hand, obtaining dynamic topography from improved mantle dynamics simulations in the future may prove feasible.

An additional lack of realism in the current model relates to the locations of subduction zones. In the current model subduction zones were largely static in their locations and generally positioned far from land. Yet in today’s world most subduction occurs adjacent to continents. Likely that was also the case during the Flood. Numerical experiments not described in this paper reveal that the patterns of water flow, erosion, and sedimentation are rather sensitive to subduction zone location. Therefore, in future studies it will be important to include more realism in subduction zone placement and to allow that placement to change dynamically.

A crucial aspect of the model that also invites further scrutiny is the locking/slipping mechanics of subducting lithosphere responsible in the model for generating the large-amplitude tsunamis. How this process may have operated during the Flood when plate speeds were so dramatically higher is far from clear. A key issue is the amount of stress the fault between the plates could have sustained without slip occurring. The reduction in rock strength associated with the runaway process in the mantle during the Flood may well have affected the lithospheric lid at the earth’s surface less than it did the mantle. If so, high stress levels in the locked plates combined with weaker rock in the mantle beneath may have worked together to yield large amplitude surface deflections between episodes of slip. Careful numerical exploration of the locking and slip mechanics of the plates in the subduction zone environment is an urgent task to be addressed in the near future.

A further deficiency in the current model is the lack of any easily eroded sediment initially present on the continental surface. That lack ought to be simple to alleviate in future studies. Hence, the numerical model described in this paper should therefore be thought of as a work in progress, as a developing framework for addressing the global-scale water flow, erosion, and sedimentation of the Flood.

CONCLUSION

Numerical simulation offers a means for investigating phenomena that are impossible, either because of their physical scale or the extreme conditions they entail, or both, to explore experimentally in a repeatable manner in the laboratory. The Genesis Flood certainly falls into this category. This paper describes a beginning attempt to apply known physical laws, physical processes that can be investigated in the laboratory, and processes on larger scales that can be studied and characterized by measurements in the present, to model important aspects of this unique cataclysmic event. The numerical model exploits the shallow water approximation to represent water flow in a thin layer on the surface of a rotating sphere corresponding to the earth. It utilizes the theory of open-channel flow to treat the suspension and transport of sediment by turbulent flowing water. As its mechanism for erosion it utilizes cavitation. To drive the water flow it draws upon a currently observable consequence of plate tectonics, namely, the locking and sudden release of the overriding lithospheric plate along its fault contact with a subducting plate in a subduction zone. Today, when the overriding plate unlocks and rebounds, its upward motion can, and often does, generate a water wave known as a tsunami. During the Flood, when plate speeds were orders of magnitude higher than they are today, the amplitudes of the tsunamis were potentially vastly larger.

In the numerical model such large-amplitude tsunamis are utilized to drive the global water flow. Along the continental margins water speeds consistently exceed the cavitation threshold, leading to intense erosion there of the continental bedrock. As the tsunamis surge onto the continental surface, the turbulent water transports the eroded sediment inland and deposits it in orderly patterns characterized by large spatial scales. When plate speeds begin to fall due to the exhaustion of gravitational energy driving the flow of rock in the mantle, the tsunamis decrease in frequency and amplitude, water velocities drop toward zero, and the water that had been pulsing across the continental surface drains back into the ocean basin. In the case highlighted in this paper, erosion and deposition rates approach those needed to account for the average sediment thickness on today’s continental surface.

This numerical model, basic as it is, sheds new light on several fundamental issues related to the Flood. It seems to account for (1) how such a huge volume of new sediment could arise during the brief time span of the Flood; (2) how the astonishingly thick columns of sediment observed so commonly in continental settings managed to be deposited on top of the normally high-standing continental surface; (3) how the vast lateral scales and horizontal

continuity of many sedimentary formations were generated; (4) possibly why current directions in Paleozoic sediments in the southwestern U. S. commonly are oriented in the WSW direction; and (5) how the detailed vertical structure of that record, often characterized by large numbers of thin beds separated by planar surfaces, arose. With more realism included in the future, the tsunami mechanism may well be able also to account for the vast regions of flat, deeply beveled Precambrian basement rock known as continental shields.

These promising results invite several future refinements and additions. Examples include a hyperconcentrated flow model at the base of the turbulent water column, dynamic migration of subduction zones, and dynamic topography arising from rapid motions of rock inside the mantle.

REFERENCES

Ager, D.V. 1973. The nature of the stratigraphical record. London: MacMillan.

Austin, S.A. (ed.) 1994. Grand Canyon: Monument to Catastrophe. Santee, CA: Institute for Creation Research.

Baumgardner, J. 2016. Numerical modeling of the large-scale erosion, sediment transport, and deposition processes of the Genesis Flood. *Answers Research Journal* 9:1-24.

Baumgardner, J.R. 2013. Explaining the continental fossil-bearing sediment record in terms of the Genesis Flood: Insights from numerical modeling of erosion, sediment transport, and deposition processes on a global scale. In *Proceedings of the Seventh International Conference on Creationism*, ed. M. Horstemeyer, Pittsburgh, Pennsylvania: Creation Science Fellowship, Inc.

Baumgardner, J. R. 2003. Catastrophic plate tectonics: the physics behind the Genesis Flood. In Proceedings of the Fifth International Conference on Creationism, ed. R. L. Ivey, Jr., pp. 113–126. Pittsburgh, Pennsylvania: Creation Science Fellowship.

Baumgardner, J. R. 1994. Computer modeling of the large-scale tectonics associated with the Genesis Flood. *Proceedings of the Third International Conference on Creationism, Technical Symposium Sessions*, ed. R. E. Walsh, pp. 49-62. Pittsburgh, Pennsylvania: Creation Science Fellowship.

Blakey, R. http://deeptimemaps.com/product-category/global-series/; https://www.youtube.com/watch?v=GGtQ1zpsdx4

Brand, L., M. Wang, and A. Chadwick. 2015. Global database of paleocurrent trends through the Phanerozoic and Precambrian. *Scientific Data* 2, 150025.

Majewski, D., D. Liermann, P. Prohl, B. Ritter, M. Buchhold, T. Hanisch, G. Paul, W. Wergen, and J. Baumgardner. 2002. The operational global icosahedral-hexagonal grid point model GME: Description and high resolution tests. *Monthly Weather Review* 130:319–338.

Olson, P., E. Reynolds, L. Hinnov, and A. Goswami. 2016. Variation of ocean sediment thickness with crustal age. *Geochemistry, Geophysics, Geosystems* 17(4):1349-1369.

Pettijohn, F.J. 1975. Sedimentary Rocks, 3rd Edition. New York: Harper and Row.

Pierson, T.C. 2005. Distinguishing between debris flows and floods from field evidence in small watersheds. USGS Fact Sheet 2004-3142, U.S. Geological Survey.

Prothero, D.R., and F. Schwab. 2004. Sedimentary geology: An introduction to sedimentary rocks and stratigraphy, 2nd Edition, pp. 12–14. New York: W.H. Freeman.

Richardson, L.F. 1920. The supply of energy from and to atmospheric eddies. *Proceedings of the Royal Society of London*, Series A, 97, no. 686:354–37.

Sherburn, J. A., J. R. Baumgardner, and M.F. Horstemeyer. 2013. New material model reveals inherent tendency in mantle minerals for runaway mantle dynamics. In *Proceedings of the Seventh International Conference on Creationism*, ed. M. Horstemeyer. Pittsburgh, Pennsylvania: Creation Science Fellowship.

Staniforth, A. and J. Cote. 1991. Semi-Lagrangian integration schemes for atmospheric models—a review. *Monthly Weather Review* 119:2206–2223.

Winston, D., and P.K. Link. 1993. Middle Proterozoic rocks of Montana, Idaho, and Washington: The Belt Supergroup. In Precambrian of the conterminous United States, eds. J. Reed, P. Simms, R. Houston, D. Rankin, P. Link, R. Van Schmus, and P. Bickford, P., pp. 487–521. Boulder, Colorado: Geological Society of America, The Geology of North America, v. C-3.

THE AUTHOR

John has a Ph.D. in geophysics and space physics from UCLA and worked at Los Alamos National Laboratory in computational physics research during most of his scientific career. Since the early 1980's he has undertaken most of the primary research undergirding the concept of catastrophic plate tectonics in connection with Noah's Flood. Beginning in 1997 he served on the Radioisotopes and the Age of the Earth (RATE) team that documented multiple independent lines of radioisotope evidence that the earth is thousands, not billions, of years old. Since 2005 he has been part of a small team that has developed Mendel's Accountant, a computer model for exploring key topics population genetics relating to the origin and history of life. John currently is a senior research associate with Logos Research Associates based in Santa Ana, California, and teaches science apologetics courses at Southern California Seminary in the San Diego area.